

RESEARCH PAPER



## A MetAP2 inhibitor blocks adipogenesis, yet improves glucose uptake in cells

Md Abu Bakkar Siddik<sup>a</sup>, Bhaskar C. Das<sup>b</sup>, Louis Weiss<sup>c</sup>, Nikhil V. Dhurandhar<sup>a</sup>, and Vijay Hegde <sup>a</sup>

<sup>a</sup>Department of Nutritional Sciences, Texas Tech University, Lubbock, TX, USA; <sup>b</sup>The Icahn School of Medicine, Department of Medicine, New York, NY, USA; <sup>c</sup>Department of Pathology, The Albert Einstein College of Medicine, New York, NY, USA

### ABSTRACT

Adipose tissue expansion involves angiogenesis to remodel its capillary network. The enzyme methionine aminopeptidase 2 (MetAP2) promotes angiogenesis. MetAP2 inhibitors suppress angiogenesis and have potential anti-obesity effect. However, impairment in adipose tissue expansion is also linked with impaired glycemic control. This study investigated the effect of BL6, a MetAP2 inhibitor, on adipogenesis and glucose disposal. To test effect on angiogenesis, Human Umbilical Vein Endothelial Cells (HUVECs) were treated with BL6 for 24h to determine tube formation. Further, to test effect on adipogenesis and glucose disposal, 3T3-L1 pre-adipocytes were treated with BL6 (0 μM, 20 μM, 50 μM or 100 μM) during differentiation. Differentiated cells were stained with Oil Red O for determining lipid accumulation, and glucose uptake assay. Protein levels and RNA expression for key genes involved in the adipogenic cascade were determined. BL6 treatment of HUVECs dose dependently blocked angiogenesis. During differentiation of pre-adipocytes, 50 μM and 100 μM BL6 significantly reduced lipid accumulation. Treatment with 100 μM BL6 significantly decreased expression of adipogenic genes. Interestingly, BL6 treatment dose dependently increased glucose uptake by 3T3-L1 cells. MetAP2 inhibitor blocks angiogenesis, attenuates adipogenesis, yet increases cellular glucose uptake. Collectively this proof of concept study supports a possible role for MetAP2 inhibitor BL6, as a putative anti-obesity therapeutic agent.

### ARTICLE HISTORY

Received 1 April 2019  
Revised 8 June 2019  
Accepted 19 June 2019

### KEYWORDS

Angiogenesis; adipogenesis; lipid accumulation; glucose uptake; MetAP2 inhibitor; fumagillin

## Introduction





Obesity is highly prevalent in many developed countries and its prevalence is increasing worldwide [1]. Obesity, characterized by excess accumulation of adipose tissue, is a complex metabolic disorder that is commonly associated with type-2 diabetes mellitus (T2D), hypertension, coronary heart disease, stroke, dyslipidemia, gallbladder disease, hepatic steatosis, sleep apnea, stroke, endometrial disorder, and cancer [1–3]. Diet and exercise remain the cornerstones of obesity management; however, it is likely that many patients will require anti-obesity drugs to reduce body weight and prevent complications [4]. Adipose tissue is highly vascularized in which the adipocytes are nourished by an extensive capillary network [5–7]. Expansion of adipogenesis requires angiogenesis [5], whereas, inadequate angiogenesis or vascular dysfunction is closely associated with many metabolic disorders [8–10].

Methionine amino peptidase 2 (MetAP2), a metalloproteinase, is a regulatory element for angiogenesis and a target molecule for anti-angiogenic compounds [11–13]. In pre-clinical models of obesity and diabetes, MetAP2 inhibitors have been shown to inhibit fat mass


expansion and improve glycemic control, and reduce food intake in mice [14–16]. These findings have paved avenues for possible therapeutic intervention of obesity and obesity-associated disorders by targeting the vascular compartment. In clinical studies of obesity, beloranib, a MetAP2 inhibitor substantially increased weight loss along with improved glycemic control [17–20]. However, in spite of these promising findings, a phase 2 clinical trial testing the long-term effects of beloranib had to be stopped early because of an imbalance of venous thromboembolism along with other adverse effects in beloranib treated individuals [21].

Collectively, these significant efficacy findings support further investigation of other MetAP2 inhibitors that might alleviate some of these risks and adverse effects previously observed. Here we report the synthesis and characterization of a novel MetAP2 inhibitor compound BL6.

Fumagillin is a natural product first isolated from *Aspergillus fumigatus* in 1949, whereas its molecular target, MetAP2, was only identified in 1997 [22]. It acts by covalently modifying His231 in the active site of MetAP2 and does not inhibit MetAP1 [22,23]. In early clinical studies, it

**CONTACT** Vijay Hegde  [Vijay.Hegde@ttu.edu](mailto:Vijay.Hegde@ttu.edu)  Nutritional Sciences Department, Texas Tech University, Lubbock, TX 79409, USA; Dr. Bhaskar C. Das  [Bhaskar.Das@msm.edu](mailto:Bhaskar.Das@msm.edu)  Departments of Medicine and Pharmacological Sciences, Icahn School of Medicine at Mount Sinai, 1468 Madison Avenue, New York, NY 10029

This article has been republished with minor changes. These changes do not impact the academic content of the article.

 Supplemental data for this article can be accessed [here](#).

© 2019 The Author(s). Published by Informa UK Limited, trading as Taylor & Francis Group.

This is an Open Access article distributed under the terms of the Creative Commons Attribution License (<http://creativecommons.org/licenses/by/4.0/>), which permits unrestricted use, distribution, and reproduction in any medium, provided the original work is properly cited.

was tested primarily for oncologic indications and as an anti-parasitic agent; it was well tolerated and associated with few adverse effects [17–19]. Later, a new derivative of fumagillin was synthesized, the fumagillin-like synthetic compound TNP-470 (AGM-1470) [14,16].

We have reshaped the chemical structure of fumagillin (Supplemental Figure 1A) to generate a boron atom containing MetAP2 inhibitor analog BL6, which is unique in nature and different in chemical structure with a different pharmacophore group (Supplemental Figure 1B). In this pilot study, we investigated the effect of BL6 on angiogenesis by measuring block to tube formation in human umbilical vein endothelial cells (HUVECs). We further examined its anti-adipogenic effect by determining the inhibition of lipid accumulation in pre-adipocytes during differentiation. Dose-dependent block to adipogenesis was confirmed by gene and protein expression. Finally, the effect of a block to adipogenesis on glucose metabolism was determined by glucose uptake assay in pre-adipocytes treated with compound BL6 during adipogenesis.

## Material and methods

Experimental outlines are described below. Details of assays are presented under ‘Techniques and Assays’ (T&A) section.

### Experiment 1: does BL6 block angiogenesis?

HUVECs (cell applications, Catalog No. 200-05n), 20,000 to 30,000 were seeded per well of a 96-well plate on matrigel (Corning, Catalog No. 356,234) to promote tube formation. Three wells of cells were seeded per group for five groups of cells; control (no treatment), control DMSO (dimethyl sulfoxide), or 20  $\mu$ M, 50  $\mu$ M or 100  $\mu$ M of BL6 in DMSO. After 24 h, each well was visualized for tube formation. Images were taken and tube length measured using the NIH image j software to determine block to angiogenesis.

### Experiment 2: does BL6 block adipogenesis?

Murine 3T3-L1 (passage 3, ATCC Catalog No. CL-173) pre-adipocyte cells were treated with increasing doses of BL6 (0  $\mu$ M, 20  $\mu$ M, 50  $\mu$ M and 100  $\mu$ M with respective DMSO controls adjusted for volume) during the adipogenesis process induced with differentiation media. Two millilitres of media, either containing BL6 or respective volume of DMSO, was added to each well. The corresponding volume of DMSO 2  $\mu$ l, 5  $\mu$ l, and 10  $\mu$ l was added per ml for treatment with 20  $\mu$ M, 50  $\mu$ M, and 100  $\mu$ M of BL6, respectively. Following differentiation for 8 days with BL6 refreshed during media change every 2 days, cells were stained with Oil Red O dye and the dye was extracted to quantify lipid accumulation as described in T&A.

### Experiment 3: Does BL6 block gene expression and molecular signalling of proteins in the adipogenic pathway?

In a parallel experiment as described in experiment 2, protein lysates from 3T3-L1 pre-adipocyte cells treated with BL6 (0  $\mu$ M, 20  $\mu$ M, 50  $\mu$ M and 100  $\mu$ M with respective DMSO controls adjusted for volume) were separated on a SDS-PAGE gel and immunoblotted for Adiponectin, peroxisome proliferator-activated receptor gamma (PPAR $\gamma$ ), C/EBP $\alpha$ , C/EBP  $\beta$ , fatty acid synthase (FAS), pAKT, and glucose transporter 4 (Glut4) proteins, which were normalized to glyceraldehyde 3-phosphate dehydrogenase (GAPDH),  $\alpha$ -tubulin or  $\beta$ -actin by western blotting. Another set of similarly treated cells were lysed following 8 days of differentiation to extract RNA to determine gene expression as described in T&A. Gene expressions of Adiponectin, PPAR $\gamma$ , SREBP1c, C/EBP $\alpha$ , C/EBP  $\beta$  and FAS were measured and normalized to that of GAPDH.

### Experiment 4: BL6 enhances cellular glucose uptake independent of a block to adipogenesis

Glucose metabolism was determined following block to adipogenesis by treating 3T3-L1 cells with 0  $\mu$ M, 20  $\mu$ M, or 100  $\mu$ M BL6 in DMSO. Cells were treated with adipogenesis inducing media as described in experiment 2. Following cell differentiation for 8 days, glucose uptake assay was conducted under basal and insulin-stimulated conditions as described in T & A.

Each experiment was repeated a minimum of 4–5 times.

## Techniques and assay

### Cell culture

#### 3T3-L1 pre-adipocyte media

Ten percent Hyclone Bovine Calf Serum Defined Iron Supplemented (Hyclone, Catalog No.SH30072.03) was used with 500 mL DMEM cells media (Cellgro, Catalog No. 10-017-CV) along with 1% antibiotic (containing penicillin and streptomycin antibiotic-antimycotic solution; SIGMA-Aldrich, Catalog No. A5955)

#### 3T3-L1 adipocytes media

Ten percent Hyclone Fetal Bovine Serum-Characterized (Hyclone Catalog No. SH30071.03) was used with 500 mL DMEM cell media (Cellgro Catalog No. 10-017-CV) with 1% antibiotic (containing penicillin and streptomycin antibiotic-antimycotic solution; SIGMA-Aldrich, Catalog No. A5955).

## Induction of adipocyte differentiation

The adipocyte differentiation medium +100 nM human insulin +1  $\mu$ M dexamethasone (Alfa Aesar, Catalog No. A17590) +250  $\mu$ M 3-isobutyl-1-methylxanthine [IBMX] (Sigma-Aldrich Catalog No. I5879) was added to 3T3-L1 cells two days post confluency. Two days later, the medium was changed to adipocyte media +0.250 nM insulin and replaced every 2 days thereafter for 8 days.

Reagents were as follows: Insulin stock solution (1 mg/ml) (Sigma-Aldrich Catalog No. 10,516), dexamethasone stock solution (3.9 mg/mL)(Alfa Aesar, Catalog # A17590), methylisobutylxanthine (3-isobutyl-1-methylxanthine) (Sigma-Aldrich Catalog No. I5879).

## Determination of lipid accumulation

Oil red O, a lipid-specific dye, was used to determine lipid accumulation in murine 3T3-L1 adipocytes as described [24]. Cells were fixed for 1 h with 10% formalin solution (Sigma-Aldrich; catalog no. HT551128), washed with water, and stained for 2 h with oil red O (EMD bioscience, San Diego, CA, USA Catalog No. 3125-12), followed by 2-3 times washing with water. The dye was extracted with isopropyl alcohol (Fisher Chemical, Catalog No. A464-4), and its absorbance was read at 510 nm.

## Synthesis of the compound BL6

### Synthesis

Compound 5 (Supplemental Figure 1B) (0.28 g, 1.00 mmol, 1.00 equivalent) was dissolved in dry dimethylformamide (DMF) (2 mL) and  $\text{CH}_2\text{Cl}_2$  (4 mL). After stirring for 1 h, oxalyl chloride ( $\text{COCl}_2$ ) was added slowly at 0°C under  $\text{N}_2$  gas. The mixture was stirred at room temperature for 1.5 h. Dichloromethane was removed carefully and dry DMF (3 mL) was added for immediate use. The DMF solution was then added to the stirred mixture of 4-aminophenyl boronic acid pinacol ester [25], triethylamine ( $\text{Et}_3\text{N}$ ) and DMF (2 mL) slowly at 0°C under  $\text{N}_2$  gas. The reaction mixture was stirred at room temperature for 3 h under  $\text{N}_2$  gas. It was quenched with saturated  $\text{NH}_4\text{Cl}$  and extracted with  $\text{EtOAc}$  (40 mL). The organic phase was washed with  $\text{H}_2\text{O}$  (15 mL  $\times$  3), satd.  $\text{NaCl}$  (10 mL), dried over  $\text{Na}_2\text{SO}_4$  and filtered. The organic layer was concentrated to get a yellow solid.

### Purification

It was further purified by silica gel column chromatography using ethyl acetate and hexane as eluents to get 0.112 g of compound BL#6 as white solid (23.0%, 0.23 mmol)

(Supplemental Figure 1(b)). Rf (ethyl acetate/n-hexane 1:5 v/v): 0.30.

## Analytical data-structure elucidation

After purification, we elucidated the structure using NMR (Nuclear Magnetic Resonance). We matched the observed value of Proton  $^1\text{H}$  and carbon  $^{13}\text{C}$  of our BL6 compound with theoretical value. These are a routine test with organic chemistry to identify the newly synthesized compounds.

$^1\text{H}$  NMR (400 MHz,  $\text{DMSO-d}_6$ )  $\delta$  10.30 (s, 1H, -NH-), 7.93 (d,  $J = 8.41$  Hz, 2H), 7.82 (d,  $J = 8.59$  Hz, 2H), 7.65 (d,  $J = 8.54$  Hz, 2H), 7.43 (d,  $J = 8.34$  Hz, 2H), 6.49 (s, 1H), 2.58 (t,  $J = 6.24$  Hz, 2H), 2.20 (q,  $J = 7.43$  Hz, 2H), 1.88 (s, 3H), 1.46 (t,  $J = 6.24$  Hz, 2H), 1.29 (s, 12H), 1.06 (s, 6H), 1.03 (t,  $J = 7.43$  Hz, 3H).  $^{13}\text{C}$  NMR (400 MHz,  $\text{DMSO-d}_6$ )  $\delta$  165.25, 147.97, 142.02, 141.68, 140.89, 134.99, 131.68, 128.83, 127.39, 126.53, 120.39, 119.10, 83.35, 38.10, 35.39, 27.29, 24.58, 22.26, 14.82, 14.54.

## Immunoblotting

Cultured cells were lysed in radioimmunoprecipitation assay buffer (RIPA) buffer (#sc-24,948; SantaCruz Biotechnology) with added protein inhibitor cocktail. Protein from the lysates was collected after centrifugation (13,000 G, 4°C, 15 min) and measured by bicinchoninic acid protein assay (#B9643, #C2284; Sigma-Aldrich). 30  $\mu$ g lysates were subjected to SDS-PAGE (7.5 or 15% polyacrylamide), and transferred to polyvinylidene difluoride membranes (#162-0177; Bio-rad), incubated with primary antibody [PPAR $\gamma$ , SantaCruz Sc-7273 (1:500), C/EBP  $\alpha$ , SantaCruz Sc-365,318 (1:500), C/EBP  $\beta$ , SantaCruz Sc-7962 (1:500), GAPDH, Cell signaling, Danvers, MA, USA 2118s (1:10,000) Adiponectin, Millipore MAB3832 (1:500), PPAR $\gamma$ , SantaCruz Sc-7273 (1:500), C/EBP  $\alpha$ , SantaCruz Sc-365,318 (1:500), C/EBP  $\beta$ , SantaCruz Sc-7962 (1:500), GAPDH, Cell signaling 2118s (1:10,000) Adiponectin, Millipore, MAB3832 (1:5000)], and then quantified by secondary antibody conjugated with horseradish peroxidase and ECL detection reagents (Amersham Biosciences, #RPN2209). Protein expression was normalized to GAPDH and total AKT, and measured by densitometry using Image J software (National Institutes of Health).

## RNA extraction and gene expression analysis

Cells grown as a monolayer in six well plates were treated with BL6 along with MDI for 8 days of differentiation period. Cells were homogenized by using 990  $\mu$ l of QIAzol Lysis Reagent (Qiagen, Cat.

No.79,306) to each well of six well plates. Total RNA was extracted using RNeasy Plus Universal Mini Kit (Qiagen) and measured by using CYTATION 3 imaging reader (BioTek, Winooski, VT). cDNA was generated from 1 µg total RNA by using iScript™ Reverse Transcription Supermix (Biorad, Cat.# 1,708,841). The following reaction protocols were used (Mastercycler, Eppendorf): 25°C for 5 min, 46°C for 20 min, 95°C for 1 min. The cDNA was diluted 1:10 with nuclease-free water and stored at -20. cDNA (at a final concentration of 10ng/µL) was amplified using iTaq Universal SYBR green supermix (Biorad,) on a CFX-Connect real-time PCR instrument (Biorad). Amplification protocol for all genes was as follows: Initial denaturing at 95°C for 2 min, 40 cycles of denaturation at 95°C for 5 s, annealing at 60°C for 30 s and completed with the following steps – 95°C for 5 s, 65°C for 5 s and 95°C for 5 s. Ct values were determined and final relative quantification was determined using the delta-delta Ct method with GAPDH and β2M as the house-keeping gene.

### Primers used for gene expression

**PPAR $\gamma$ -F-** TGGAAATTAGATGACAGTGAAGTGG;  
**PPAR $\gamma$ -R-** GAGCACCTTGGCGAACAG, **Adiponec**  
**tin-F-** GCTCTCCTGTTCTCTTAATCCT; **Adip**  
**onectin-R-** AGTGCCATCTCTGCCATCA, **C/E**  
**BP  $\alpha$ -F-** AGTAACCTTGTGCCTTGGA; **C/EBP  $\alpha$ -R-**  
**GCTTCCTGTATCTTCCTCCT,** **MetAP2-F-**  
**AGATACGACAGATAACCTCAGATT;** **MetAP**  
**2-R-** AACCTTCCTCAACTATACTCCTT, **C/E**  
**BP  $\beta$ -F-** CTGAGCGACGAGTACAAGAT; **C/EB**  
**P  $\beta$ -R-** GCTGCTCCACCTTCTTCT, **Glut**  
**4-F-** CCAGCCTACGCCACCATA; **Glut**  
**4-R-** GTTCCAGCAGCAGCAGAG, **FASn**  
**-F-** TGGCTCACAGTTAAGAGTTCA; **FA**  
**Sn-R-** GCCTCCTTGATATAATCCTTCTG, **SREB**  
**P 1-F-** GCTTCTCTTCTGCTTCTCTG; **SRE**  
**BP 1-R-** GGCTGTAGGATGGTGAGT, **GAP**  
**DH-F-** GGTGAAGGTCGGTGTGAAC; **GAPDH-R-**  
**TGAGTGGAGTCATACTGGAACA.**

### Glucose uptake

As previously described [26,27], 3T3-L1 cells, treated with BL6 for 8 days during the differentiation period as described in experiment 2, were exposed to serum-free media for 2 h, then washed twice with PBS, followed by 112.5 µL Krebs-Ringer phosphate buffer treatment (136 mM NaCl, 4.7 mM KCl, 10 mM NaPO<sub>4</sub>, 0.9 mM CaCl<sub>2</sub>, 0.9mM MgSO<sub>4</sub>). To determine non-specific

glucose uptake, one well of cells was treated with 100 nM cytochalasin B (#6762, Sigma Aldrich). Next, 12.5 µL of 10X isotope solution was added to each well to a final concentration of 100 nM 2-deoxyglucose and 0.5 µCi ml<sup>-1</sup> [3H]-2-deoxyglucose (#NEC720A250UC, PerkinElmer) for 5 min. Cells were immediately washed in ice-cold PBS. Next, 500 µL of 0.05% SDS was added to each well, and incubated at 37°C for 30 min. 450 µL of cell lysate from each well was added to individual scintillation vials. The remaining 50 µL cell lysate was used for protein determination with BCA assay. The scintillation counts per minute were normalized to the protein content of each well.

### Statistics

All values are expressed as mean ± standard deviation (SD). The glucose uptake and signalling experiments were repeated three times or more, and similar results were obtained. Statistical differences between two group means were determined by Student's *t* test, and the differences were considered significant at *p* < 0.05. One-way ANOVA was used for multiple comparisons followed by tukey's test. Groups not sharing a letter denote statistical significance. Significance was considered at *p* < 0.05.

### Results

#### Experiment 1: BL6 blocks angiogenesis

To determine the ability of MetAP2 inhibitor compound BL6 to block angiogenesis, 20,000 or 30,000 HUVECs were treated with increasing doses of the compound. We first tested 0 µM, 100 µM, 200 µM, and 1 mM compound BL6 on 20,000 HUVECs and found 200 µM and 1 mM to be toxic to cells (data not shown). Therefore, we used 0 µM, 20 µM, 50 µM, and 100 µM for subsequent testing. HUVECs show visual disruption in tube formation with 20 µM and 50 µM of BL6 (Figure 1(a,b)). There appears to be some block to tube formation by DMSO alone when compared with no DMSO control cells (Figure 1(a,b)). Therefore, cells treated with different concentrations of BL6 were compared to their respective DMSO controls adjusted for volume. However, despite the DMSO effect, inhibition of tube formation by different concentrations of BL6 is visually evident. Treatment with 100µM BL6 did not show any visually observable tube formation; therefore, tube formations in these cells were not quantified (Figure 1(a,b)).

To quantify tube formation, tube length was measured using the Image j software. Both 20,000 and 30,000 HUVECs show a significant reduction in total

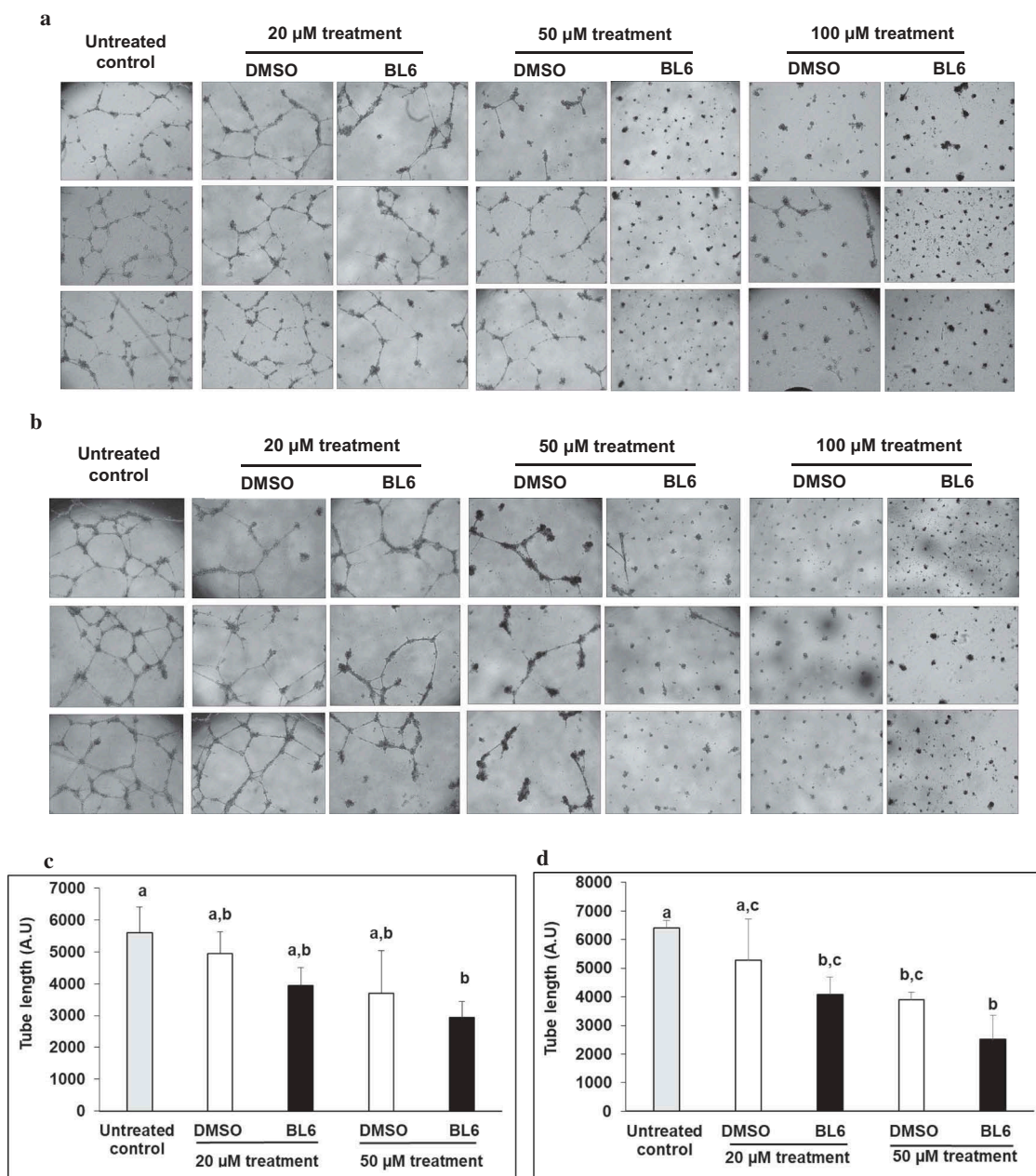


**Figure 1.** Block to angiogenesis measured by tube formation in HUVECs. 20,000 (a) and 30,000 (b) cells were treated with 20  $\mu\text{M}$ , 50  $\mu\text{M}$  and 100  $\mu\text{M}$  of BL6 and their respective tube length measured (c, d). Cells were cultured for 24 hours on Matrigel at 37°C and tube formation was determined following 24 hours. The effect of each dose of BL6 was compared to its own DMSO control. The experiment was repeated a minimum of three times.

tube length when treated with 20  $\mu\text{M}$ , and 50  $\mu\text{M}$  of the anti-angiogenic compound BL6 (Figure 1(c,d)).

### Experiment 2: BL6 blocks adipogenesis

To determine if dose-dependent block to angiogenesis by BL6 also blocks adipogenesis and lipid accumulation, 3T3-L1 cells were treated with increasing doses of BL6 (0  $\mu\text{M}$ , 20  $\mu\text{M}$ , 50  $\mu\text{M}$  and 100  $\mu\text{M}$  of BL6 along

with corresponding DMSO control adjusted for volume) during differentiation with MDI cocktail (Figure 2(a)). Following differentiation for 8 days, cells were stained with oil red O dye and the dye was extracted to quantify lipid accumulation. In a dose-dependent manner, BL6 significantly blocks adipogenesis as indicated by lipid accumulation (Figure 2(b)). To determine if compound BL6 can block adipogenesis and lipid accumulation after differentiation is induced, we treated 3T3-L1 cells with BL6, 2 days following

adipogenesis induction with MDI cocktail. We observed block to adipogenesis and lower lipid accumulation (20  $\mu\text{M}$   $p = 0.06$ ; 100  $\mu\text{M}$   $p < 0.005$ ) (data not shown). Changes in gene and protein expression with these observations will be determined in future studies. In the current study further analysis was done treating cells with compound BL6 along with MDI cocktail during differentiation.

### Experiment 3: (a) BL6 down-regulates the expression of adipogenic genes

To determine changes in gene expression by BL6 treatment, quantitative real-time polymerase chain reaction (RT-PCR) was performed. RNA extracted from 3T3-L1

cells treated with BL6 (0  $\mu\text{M}$ , 20  $\mu\text{M}$ , 50  $\mu\text{M}$  and 100  $\mu\text{M}$ ) during differentiation was used to determine the expression of MetAP2, PPAR $\gamma$ , FAS, adiponectin, SREBP1, C/EBP- $\beta$  and C/EBP $\alpha$ . We first determined gene expression of the MetAP2 gene in these cells following BL6 treatment, which is down-regulated in a dose-dependent manner as expected (Figure 3). Treatment with 100  $\mu\text{M}$  of BL6 shows significantly reduced expression of FAS, SREBP1, and C/EBP  $\alpha$  compared with DMSO treated cells (Figure 3(c)). Furthermore, PPAR $\gamma$ , C/EBP  $\beta$  and adiponectin involved in the adipogenic pathway were also lower by approximately 30% further confirming block to adipogenesis by MetAP2 inhibitor BL6, but the difference was not statistically significantly different.

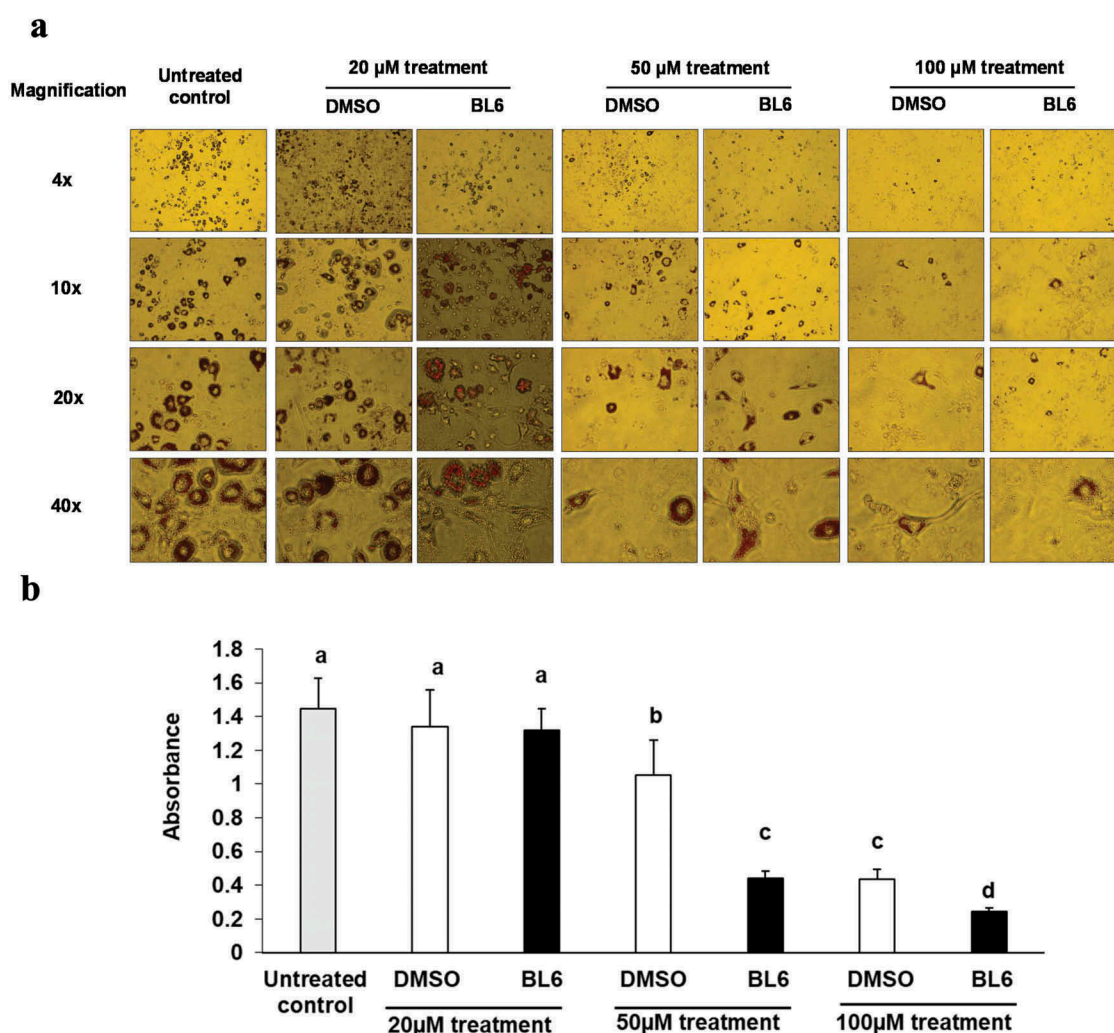


**Figure 2.** Effect of BL6 on adipocyte differentiation (a) and corresponding Oil Red O staining (b) in cultured 3T3-L1 adipocytes. (a) 3T3-L1 pre-adipocyte cells were treated with 20  $\mu\text{M}$ , 50  $\mu\text{M}$  and 100  $\mu\text{M}$  of BL6 along with MDI for 8 days during differentiation. Block to adipogenesis was visually observed following oil red O staining for lipid. (b) Lipid staining was quantified by measuring absorbance. Y-axis shows absorbance of Oil Red O dye at 510 nm. Data are presented as average absorbance  $\pm$  sd ( $n = 6$ ). The effect of each dose of BL6 was compared to its own DMSO control. Groups sharing different alphabet denote statistical significance ( $P < 0.05$ ). The experiment was repeated a minimum of three times.

**(b) protein expression of adipogenic genes increased following treatment with BL6 compared with untreated control**

Cellular protein lysates were extracted from 3T3-L1 cells treated with BL6 (0  $\mu$ M, 20  $\mu$ M, 50  $\mu$ M and 100  $\mu$ M) for 8 days during differentiation to determine changes in molecular signalling by western blotting analysis. Genes involved in the adipogenic pathway (Figures 4 and 5), PPAR $\gamma$  (A), C/EBP  $\alpha$  (B), FAS (C), and adiponectin (D) all showed significantly increased protein expression despite block to adipogenesis and lipid accumulation. Immunoblotting for genes playing a role in cellular glucose uptake showed a dose-dependent increase in pAKT expression with 20  $\mu$ M and 50  $\mu$ M compound BL6 treatment (Figure 4(e)) and a highly significant increase in Glut4

abundance for all three doses of MetAP2 inhibitor treatment (Figures 4 and 5(f)).

**Experiment 4: BL6 enhances cellular glucose uptake independent of adipogenesis**

To determine glucose metabolism following a reduction in adipogenesis, murine 3T3-L1 cells were treated with 0  $\mu$ M, 20  $\mu$ M or 100  $\mu$ M BL6 during differentiation with MDI. Cells were differentiated for 8 days followed by glucose uptake assay. We first determined insulin independent effect of BL6 on cellular glucose uptake in cells treated with 100  $\mu$ M dose during differentiation. As seen in Figure 6(a), compared to volume-adjusted DMSO treated control cells, BL6-treated cells significantly ( $p < 0.05$ )

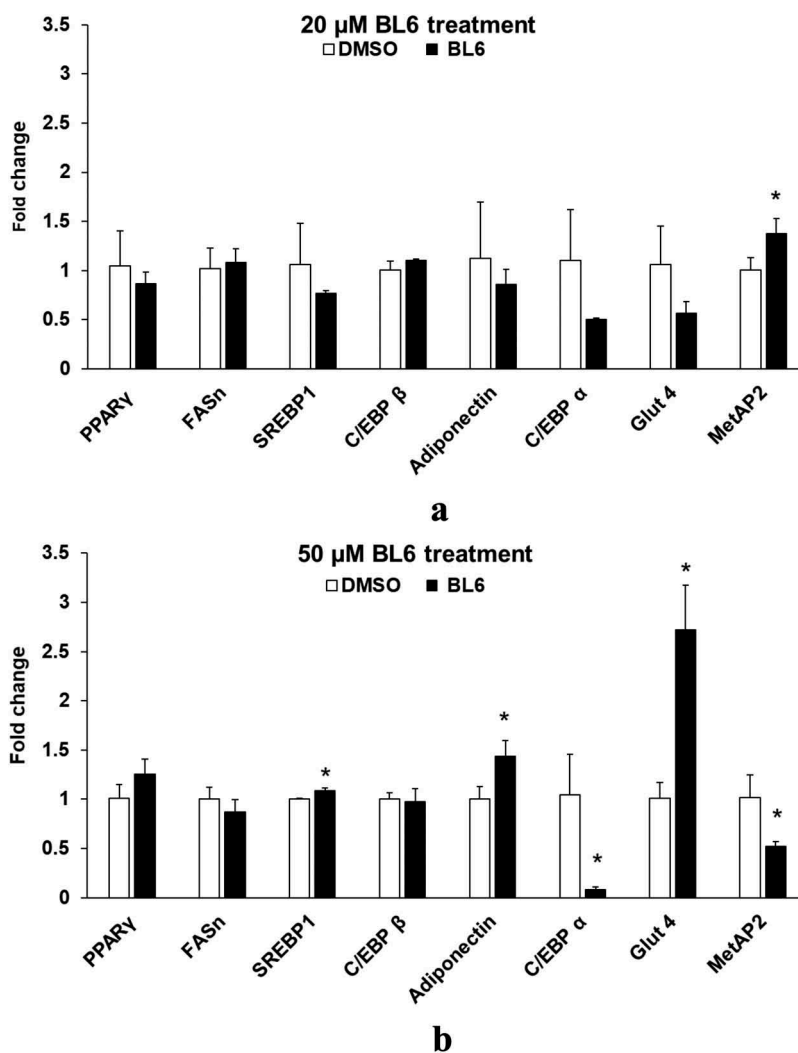


**Figure 3.** Gene expression of PPAR $\gamma$ , FASn, SREBP1, C/EBP  $\beta$ , adiponectin, C/EBP  $\alpha$ , Glut4 and MetAP2 for 20  $\mu$ M (a), 50  $\mu$ M (b) and 100  $\mu$ M (c) of BL6 treatment along with their respective DMSO control. Real time qRT-PCR was performed to determine the relative gene expression following BL6 treatment. The Y-axis shows fold-change difference in expression. The effect for each dose of BL6 was compared to its own DMSO control. Data are presented as average fold change  $\pm$  sd ( $n = 3$ ). Bars showing asterisks on top denote statistical significance ( $P < 0.05$ ). The experiment was repeated a minimum of three times.

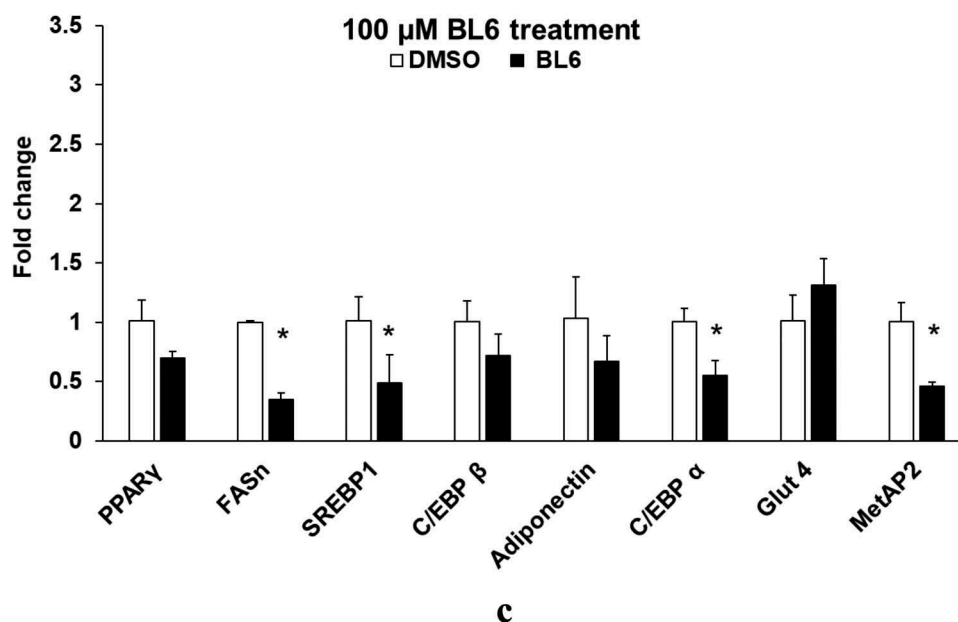


Figure 3. Continued

increase glucose uptake and similar levels to insulin-treated cells (Figure 6(a)). Next, we determined if block to adipogenesis affects insulin-stimulated glucose uptake. BL6 treatment dose-dependently increased glucose uptake compared with DMSO treated control cells and insulin-stimulated control cells (Figure 6(b),  $p < 0.05$  as determined by ANOVA). The basal group represents glucose uptake by control adipocytes, whereas Insulin stimulation shows approximately a 14-fold higher glucose uptake in adipocytes (second bar from the left, Figure 6(b)). Increase in glucose uptake observed in treated cells suggests that despite the reduction in adipogenesis by BL6, these cells are metabolically healthy and improve glucose metabolism.

## Discussion

Obesity is a serious chronic disease that is linked with excess accumulation of adipose tissue and consequential metabolic and other health disorders, including insulin resistance, impaired glycemic control or diabetes. The expansion of adipose tissue is accompanied by the development of vasculature, as adipogenesis is tightly associated with angiogenesis [28]. Adipose tissue produces and secretes many different types of pro- and anti-angiogenic factors [29]. Several *in vivo* studies have proposed that inhibition of the development of the vascular network in adipose tissue may establish an anti-obesity therapy [14,16,29–31]. Angiogenesis inhibitors fumagillin and its chemical analog TNP-470 impair adipose tissue growth in mice by selectively inhibiting endothelial cell growth via suppression of methionine aminopeptidase [14,16]. On the other

hand, some animal models suggest that restricting adipose tissue expansion may have a deleterious effect on glucose metabolism. Therefore, it would be important to consider glucose disposal, when angiogenesis inhibitors are tested as inhibitors of adipogenesis. It would be highly desirable if an angiogenic inhibitor reduces adipogenesis without reducing glucose uptake by adipose tissue.

In the current *in vitro* study, we evaluated the anti-angiogenic and anti-adipogenic property of a boron-based chemical compound BL6, for its potential development as an anti-obesity drug. We examined the effect of BL6 as an angiogenic inhibitor in HUVECs during tube formation. We also investigated the effect of BL6 on adipogenesis *in vitro* during differentiation of 3T3-L1 pre-adipocytes and regulation of adipogenic protein and gene expression. Glucose uptake by BL6-treated 3T3-L1 adipocytes was further determined by glucose uptake assay.

BL6 dose-dependently reduced angiogenesis in HUVECs (Figure 1) and adipogenesis in 3T3-L1 cells (Figure 2). In 3T3-L1 cells, BL6 significantly suppressed differentiation from pre-adipocytes to adipocytes as determined by oil Red O staining, which specifically stains triglycerides proportional to cell differentiation or lipid accumulation [24]. We did not observe any difference in lipid accumulation with 20  $\mu$ M BL6 compared with its DMSO treated control, but both 50  $\mu$ M and 100  $\mu$ M concentration of BL6 suppressed lipid accumulation significantly ( $P < 0.05$ ) (Figure 2(a,b)). In contrast, a previous *in vitro* study demonstrated higher differentiation rate of pre-adipocytes to adipocytes when treated with the natural



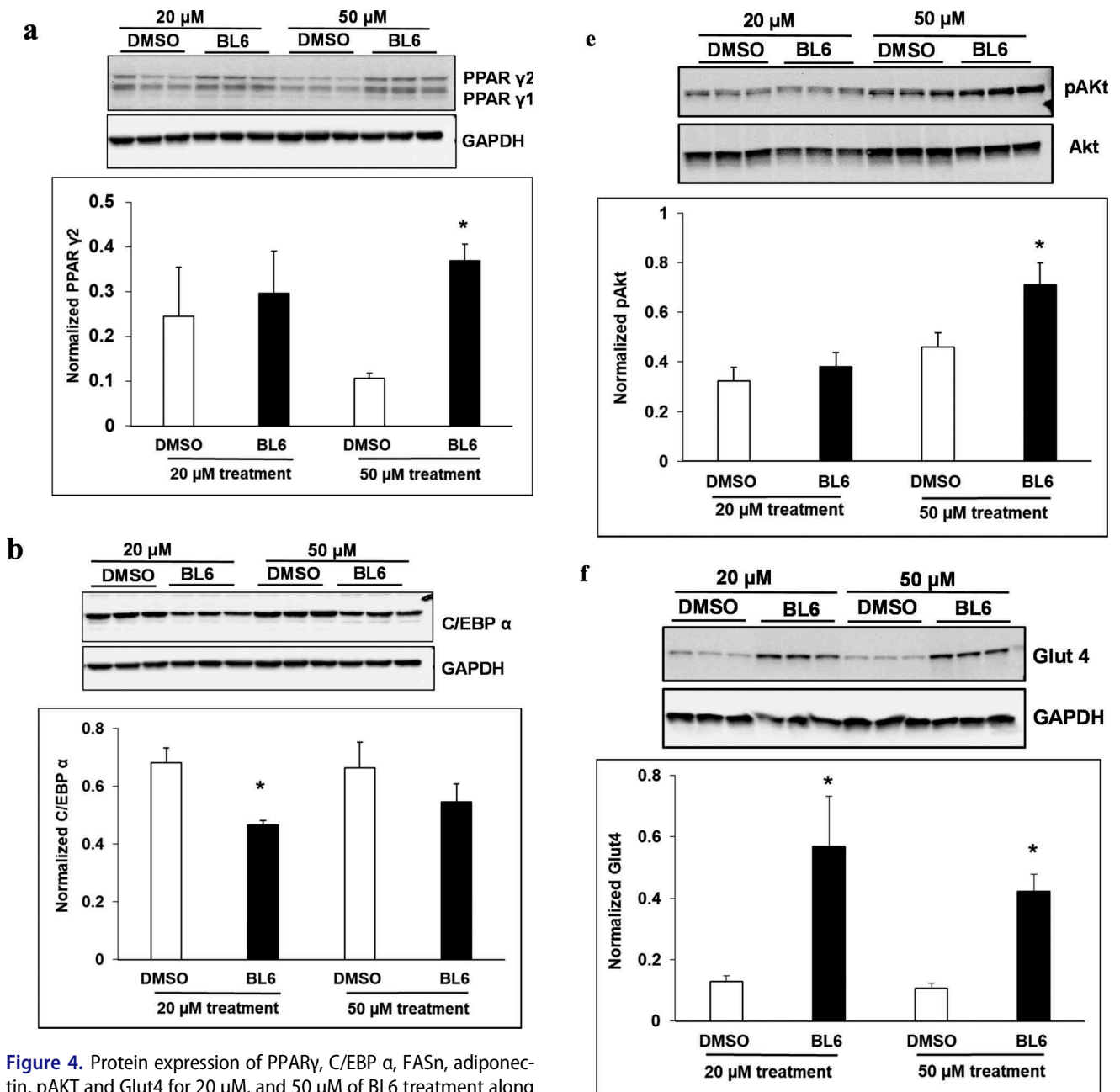


**Figure 4.** Protein expression of PPAR $\gamma$ , C/EBP  $\alpha$ , FASN, adiponectin, pAKT and Glut4 for 20  $\mu$ M, and 50  $\mu$ M of BL6 treatment along with DMSO control. Protein lysates from 3T3-L1 cells treated with 20  $\mu$ M BL6, and 50  $\mu$ M BL6 during differentiation were separated on a SDS-PAGE gel, transferred onto a nitrocellulose membrane and immunoblotted with PPAR $\gamma$ , C/EBP $\alpha$ , FASN, adiponectin, pAKT, Glut4 and GAPDH antibodies. Graphs show average density of protein bands normalized to GAPDH and Akt. The effect of each dose of BL6 was compared to its own DMSO control. Data are presented as average  $\pm$  sd ( $n = 3$ ). Statistical significance was determined by Student TTEST ( $P < 0.05$ ) and shown by asterisks on top of the bar.

angiogenic inhibitor, fumagillin [32]. However, fumagillin and its analog derivative TNP-470, have been shown to have inconsistent anti-obesity effects *in vivo* [33,34]. Thus, there appears to be differences with the anti-adipogenic potential of fumagillin and its derivative [14]. Oil Red

**Figure 4.** Continued

O stained microscopic images also showed smaller and fragmented lipid droplets within adipocytes treated with 100  $\mu$ M of BL6 compared with control. This suggests that compound BL6 may also affect the formation of the structural protein coating lipid droplets, such as perilipin [35].

BL6 reduces adiponectin gene expression in 3T3-L1 adipocytes, which supports the lower adipogenic differentiation or lipid accumulation observed. However, in the presence of BL6, protein translation for adiponectin was higher compared to control cells. BL6 suppresses PPAR $\gamma$  gene expression, the master regulator of adipocyte differentiation, at the higher 100  $\mu$ M dose, but not with 20  $\mu$ M or

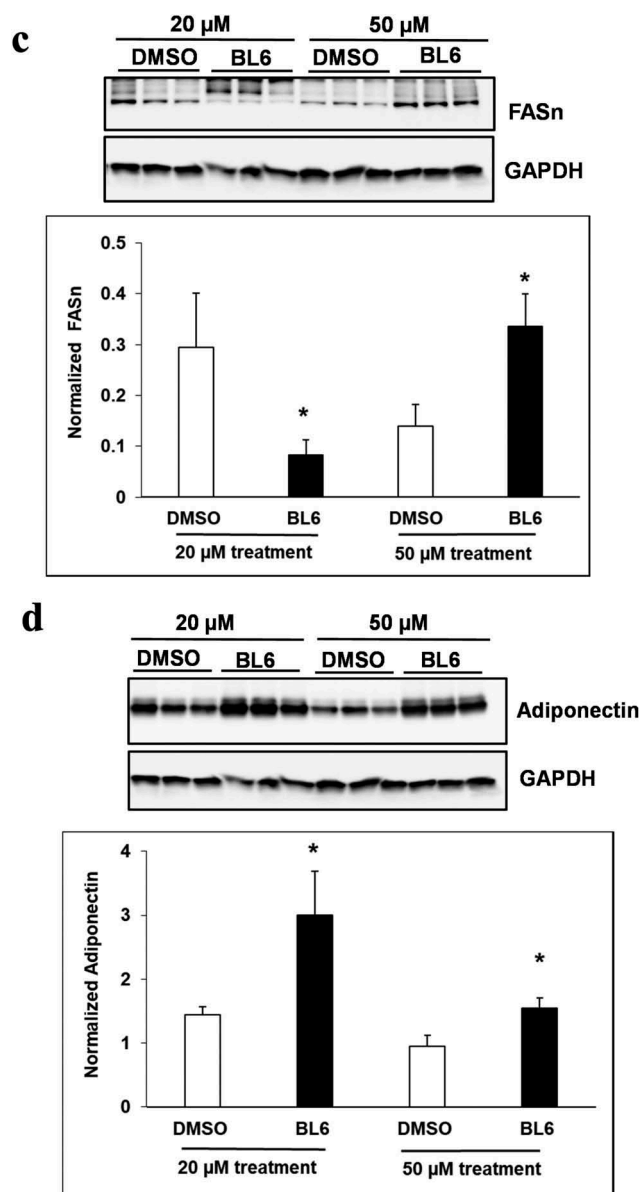


Figure 4. Continued

50  $\mu$ M dose. SREBP1, an upstream molecule of PPAR $\gamma$ , which regulates PPAR $\gamma$  expression and FAS a molecule downstream from PPAR $\gamma$  are both significantly down-regulated by treatment with 100  $\mu$ M BL6. This suggests that BL6 suppresses PPAR $\gamma$  directly or through down-regulation of SREBP1 and affects adipocyte differentiation via downregulation of FAS expression. Reduced level of FAS expression is consistent with our oil Red O data showing less lipid accumulation.

Interestingly, BL6 did not significantly influence the C/EBP  $\beta$  gene expression. C/EBP  $\beta$  is an early regulator of adipocyte differentiation and we collected protein and RNA following 8 days of cellular differentiation, this might explain the lack of observable change with C/EBP  $\beta$  expression by day 8 [36].

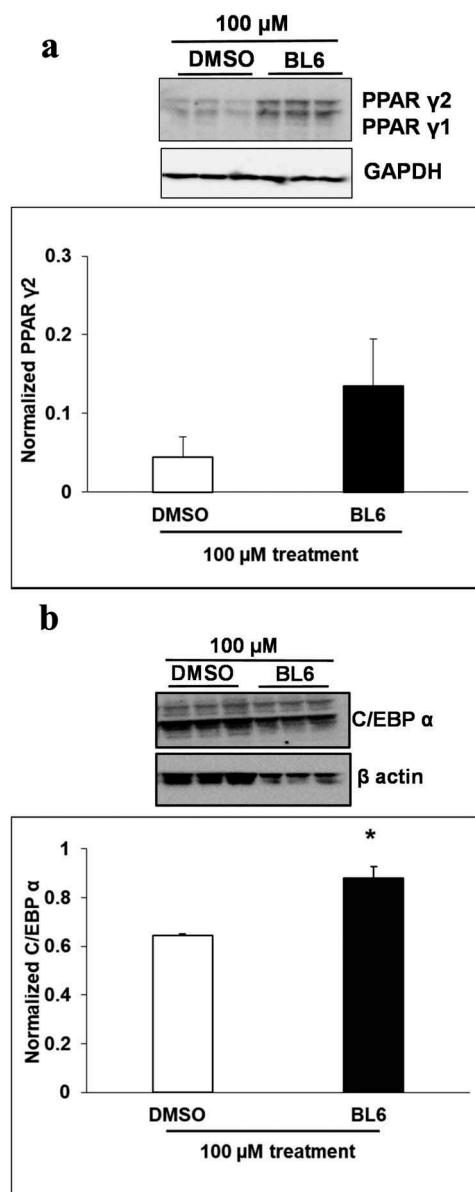


Figure 5. Protein expression of PPAR $\gamma$ , C/EBP  $\alpha$ , FASn, adiponectin, pAKT and Glut4 for 100  $\mu$ M of BL6 treatment along with DMSO control. Protein lysates from 3T3-L1 cells treated with 100  $\mu$ M BL6 during differentiation were separated on a SDS-PAGE gel, transferred onto a nitrocellulose membrane and immunoblotted with PPAR $\gamma$ , C/EBP  $\alpha$ , FAS, adiponectin, pAKT, Glut4,  $\beta$  actin,  $\alpha$  tubulin, and GAPDH antibodies. Graphs show average density of protein bands normalized to either GAPDH,  $\beta$  actin or  $\alpha$  tubulin. The effect of 100 $\mu$ M BL6 on protein expression was compared to its own DMSO control. Data are presented as average  $\pm$  sd (n = 3). Statistical significance was determined by Student TTEST (P < 0.05) and shown by asterisks on top of the bar. The experiment was repeated a minimum of three times.

C/EBP $\alpha$ , a member of the self-regulatory loop with PPAR $\gamma$ , is also significantly suppressed by 100 $\mu$ M BL6. Despite the reduction in adipogenesis, BL6 significantly increases cellular glucose uptake in 3T3-L1 cells in

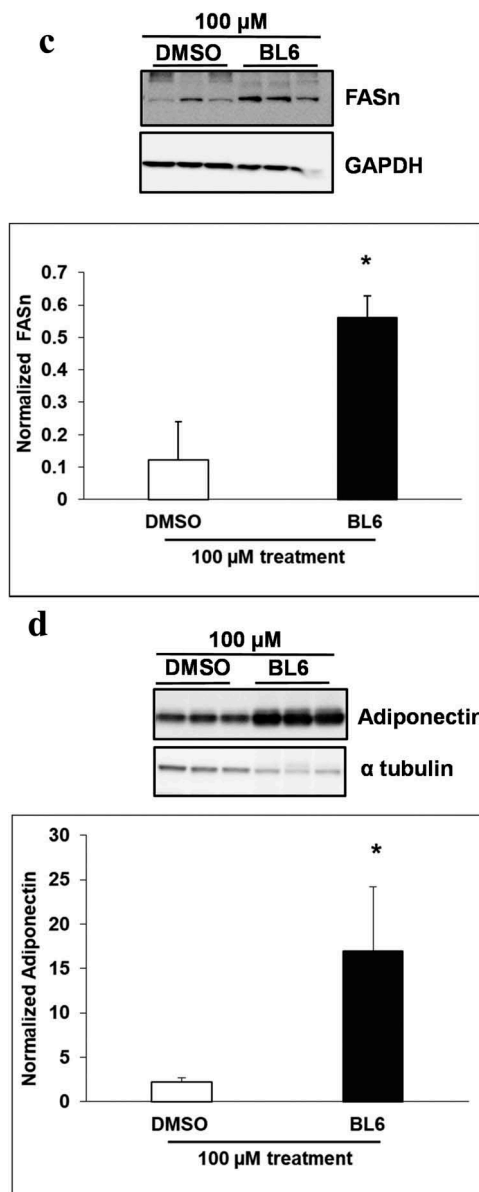


Figure 5. Continued

a dose-dependent manner (Figure 6). C/EBP $\alpha$  improves insulin sensitivity by upregulating insulin receptor (IR) insulin receptor substrate-1 (IRS-1) and Glut4 [37] and Wu Z et al. suggested that PPAR $\gamma$  alone can induce Glut 4 in absence of C/EBP $\alpha$  [38]. Therefore, the non-significant effect of BL6 on PPAR $\gamma$  expression may positively affect glucose uptake in these cells. This suggests improvement in glucose metabolism despite impaired adipogenesis and adiponectin secretion, which would be important for future in vivo studies and developing BL6 for therapeutic use.

DMSO treatment itself inhibits the expression of adipocyte phenotype and expression of adipogenic genes [39], which may affect our ability to observe significant differences at lower concentrations of BL6.

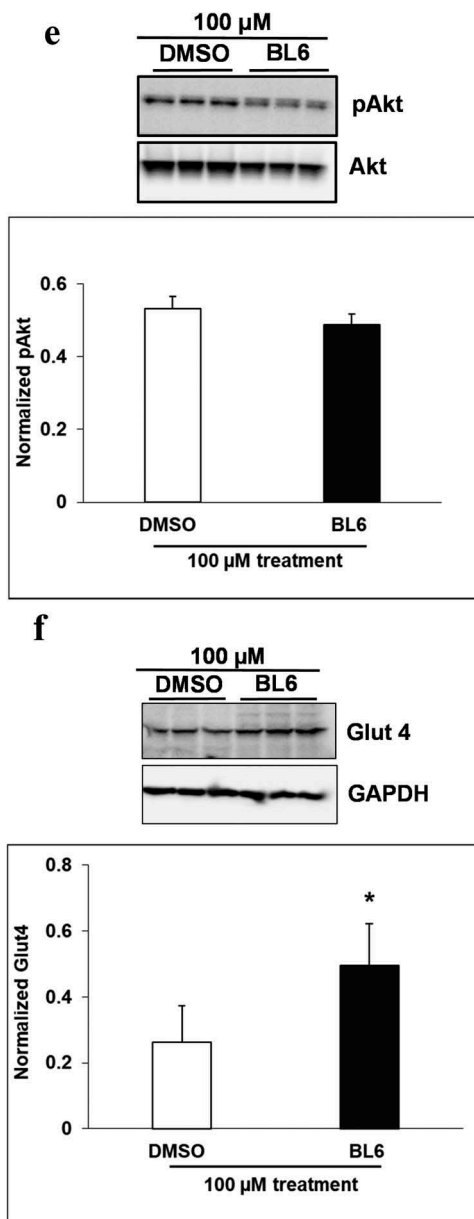
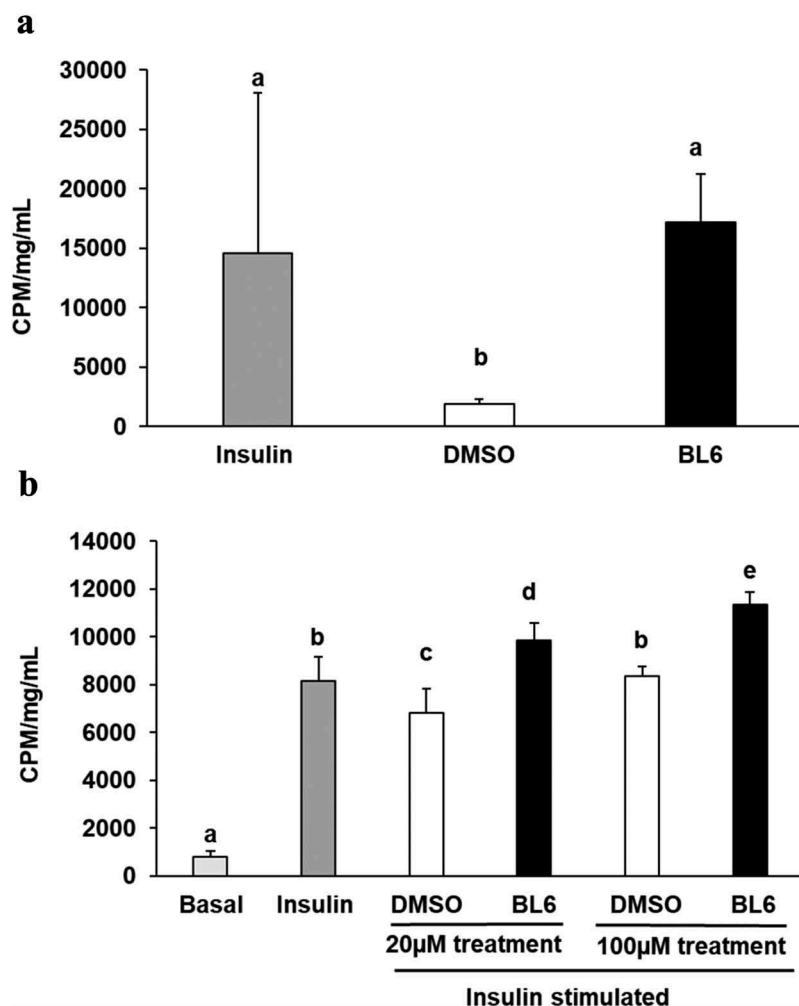


Figure 5. Continued

To capture the true effect of compound BL6, we have compared the different BL6 dose-treated cells to its respective DMSO volume control and measured statistically differences between the two groups.

Interestingly, despite a significant reduction in adipogenic gene expression, we observed a contradictory increase in protein translation (Figures 4 and 5). The increased protein translation for pAKT, Glut4 and adiponectin support concurrent dose-dependent increase in cellular glucose uptake in these cells. The results obtained are not in error as independent experiments have shown similar results, but the observed dichotomy between RNA and protein expressions for the same gene could be due to several reasons, including an effect



**Figure 6.** Glucose uptake for 20  $\mu$ M and 100  $\mu$ M of BL6 treated adipocyte cells. 3T3-L1 pre-adipocyte cells were treated with 20  $\mu$ M, and 100  $\mu$ M of BL6 along with MDI for 8 days during differentiation. Glucose uptake assay was performed following differentiation. (a) Insulin independent glucose uptake was determined with 100 $\mu$ M BL6 treated cells. Y-axis represents glucose uptake in CPM/mg/mL. (b) Similarly the effect of insulin during block to adipogenesis when cells were treated with 20 $\mu$ M and 100  $\mu$ M of BL6 was determined under insulin stimulated conditions. Basal group on the X-axis represents glucose uptake independent of insulin. Radioactive glucose uptake was normalized to total protein content. Data are presented as average  $\pm$  sd (n = 6). Groups sharing different alphabet denotes statistical significance (P < 0.05) as determined by ANOVA. The experiment was repeated a minimum of three times.

on protein ubiquitination, that would prevent protein degradation or protein stability may be increased due to post-translational modifications like phosphorylation, acetylation, and glycosylation, or the protein may be a long-lived protein which gets accumulated over time while the mRNA turnover is quick [40].

In conclusion, inhibition of MetAP2, a regulatory element for angiogenesis and a target molecule for anti-angiogenic compounds are a promising approach to treating diabetes, obesity, and associated metabolic disorders. Pre-clinical and clinical studies have shown, inhibition of fat mass expansion and improved glycaemic control by MetAP2 inhibitors [14–20]. These findings suggest a possible therapeutic intervention of obesity and obesity-associated disorders by targeting

the vascular compartment. However, a long-term phase 2 clinical trial with beloranib, a MetAP2 inhibitor was associated with venous thrombotic adverse events likely resulting from drug effects on vascular endothelial cells (ECs) [21]. Promising findings observed with various studies support further investigation of other MetAP2 inhibitors that might alleviate some of these risks and adverse effects previously observed. ZGN-1061, a MetAP2 inhibitor with improved safety profile and anti-diabetic properties than beloranib in mice [41] is in clinical development. In this study, compound BL6 blocks angiogenesis and adipogenesis *in vitro* yet improve cellular glucose uptake warranting future *in vivo* analysis of its safety and efficacy to develop as a possible anti-obesity therapeutic agent.

## Acknowledgments

Competing interest: Patent for compound BL#6 has been applied and is currently pending (BD, LW, ND, VH)

## Author Contributions

AS: Conducted experiments, analyzed and prepared results, helped in writing manuscript.

BD: Participated in data analysis, interpretation and manuscript preparation.

LW: Participated in data analysis, interpretation and manuscript preparation.

ND: Helped with study design, participated in data analysis, interpreted data and manuscript preparation.

VH: Designed and conducted the study, helped in troubleshooting, participated in data analysis, interpreted data and prepared manuscript draft.

## Disclosure statement

No potential conflict of interest was reported by the authors.

## ORCID

Vijay Hegde  <http://orcid.org/0000-0003-4160-2764>

## References

- [1] Kopelman PG. Obesity as a medical problem. *Nature*. 2000;404(6778):635–643.
- [2] Friedman JM. Obesity in the new millennium. *Nature*. 2000;404(6778):632–634.
- [3] Roth J, Qiang X, Marban SL, et al. The obesity pandemic: where have we been and where are we going? *Obes Res*. 2004;12(Suppl 2):88S–101S.
- [4] Bray GA, Tartaglia LA. Medicinal strategies in the treatment of obesity. *Nature*. 2000;404(6778):672–677.
- [5] Bouloumie A, Lolmede K, Sengenès C, et al. Angiogenesis in adipose tissue. *Ann Endocrinol (Paris)*. 2002;63(2 Pt 1):91–95.
- [6] Crandall DL, Hausman GJ, Kral JG. A review of the microcirculation of adipose tissue: anatomic, metabolic, and angiogenic perspectives. *Microcirculation*. 1997;4(2):211–232.
- [7] Silverman KJ, Lund DP, Zetter BR, et al. Angiogenic activity of adipose tissue. *Biochem Biophys Res Commun*. 1988;153(1):347–352.
- [8] Soares R. Angiogenesis in diabetes. *Unraveling the angiogenic paradox*. *The Open Circ Vascular J* 2010; 3: 3–9.
- [9] Costa R, Rodrigues I, Guardao L, et al. Modulation of VEGF signaling in a mouse model of diabetes by xanthohumol and 8-prenylnaringenin: unveiling the angiogenic paradox and metabolism interplay. *Mol Nutr Food Res*. 2017;61(4).
- [10] Soares R. Angiogenesis in the metabolic syndrome. In: Soares R, Costa C, editors. *Oxidative stress, inflammation and angiogenesis in the metabolic syndrome*. Dordrecht (Netherlands): Springer Sci Business Media; 2009. p. 85–99.
- [11] Ingber D, Fujita T, Kishimoto S, et al. Synthetic analogues of fumagillin that inhibit angiogenesis and suppress tumour growth. *Nature*. 1990;348(6301):555.
- [12] Griffith EC, Su Z, Turk BE, et al. Methionine aminopeptidase (type 2) is the common target for angiogenesis inhibitors AGM-1470 and ovalicin. *Chem Biol*. 1997;4(6):461–471.
- [13] Selvakumar P, Lakshmi Kuttamma A, Dimmock JR, et al. Methionine aminopeptidase 2 and cancer. *Biochim Biophys Acta (BBA)- Rev Cancer*. 2006;1765(2):148–154.
- [14] Brakenhielm E, Cao R, Gao B, et al. Angiogenesis inhibitor, TNP-470, prevents diet-induced and genetic obesity in mice. *Circ Res*. 2004;94(12):1579–1588.
- [15] Neels JG, Thinnen T, Loskutoff DJ. Angiogenesis in an in vivo model of adipose tissue development. *Faseb J*. 2004;18(9):983–985.
- [16] Rupnick MA, Panigrahy D, Zhang CY, et al. Adipose tissue mass can be regulated through the vasculature. *Proc Natl Acad Sci U S A*. 2002;99(16):10730–10735.
- [17] Hughes TE, Kim DD, Marjason J, et al. Ascending dose-controlled trial of beloranib, a novel obesity treatment for safety, tolerability, and weight loss in obese women. *Obesity (Silver Spring)*. 2013;21(9):1782–1788.
- [18] Kim DD, Krishnarajah J, Lillioja S, et al. Efficacy and safety of beloranib for weight loss in obese adults: a randomized controlled trial. *Diabetes Obes Metab*. 2015;17(6):566–572.
- [19] McCandless SE, Yanovski JA, Miller J, et al. Effects of MetAP2 inhibition on hyperphagia and body weight in Prader-Willi syndrome: A randomized, double-blind, placebo-controlled trial. *Diabetes Obes Metab*. 2017;19(12):1751–1761.
- [20] Shoemaker A, Proietto J, Abuzzahab MJ, et al. A randomized, placebo-controlled trial of beloranib for the treatment of hypothalamic injury-associated obesity. *Diabetes Obes Metab*. 2017;19(8):1165–1170.
- [21] Proietto J, Malloy J, Zhuang D, et al. Efficacy and safety of methionine aminopeptidase 2 inhibition in type 2 diabetes: a randomized, placebo-controlled clinical trial. *Diabetologia*. 2018.
- [22] Liu S, Widom J, Kemp CW, et al. Structure of human methionine aminopeptidase-2 complexed with fumagillin. *Science*. 1998;282(5392):1324–1327.
- [23] Sin N, Meng L, Wang MQ, et al. The anti-angiogenic agent fumagillin covalently binds and inhibits the methionine aminopeptidase, MetAP-2. *Proc Natl Acad Sci U S A*. 1997;94(12):6099–6103.
- [24] Ramirez-Zacarias JL, Castro-Munozledo F, Kuri-Harcuch W. Quantitation of adipose conversion and triglycerides by staining intracytoplasmic lipids with Oil red O. *Histochemistry*. 1992;97(6):493–497.
- [25] Das BC, Thapa P, Karki R, et al. Boron chemicals in diagnosis and therapeutics. *Future Med Chem*. 2013;5(6):653–676.
- [26] Dhurandhar EJ, Dubuisson O, Mashtalir N, et al. E4orf1: a novel ligand that improves glucose disposal in cell culture. *PLoS One*. 2011;6(8):e23394.
- [27] Na HN, Hegde V, Dubuisson O, et al. E4orf1 enhances glucose uptake independent of proximal insulin signaling. *PLoS One*. 2016;11(8):e0161275.
- [28] Cao Y. Angiogenesis modulates adipogenesis and obesity. *J Clin Invest*. 2007;117(9):2362–2368.

- [29] Lijnen HR. Angiogenesis and obesity. *Cardiovasc Res.* **2008**;78(2):286–293.
- [30] Kim YM, An JJ, Jin YJ, et al. Assessment of the anti-obesity effects of the TNP-470 analog, CKD-732. *J Mol Endocrinol.* **2007**;38(4):455–465.
- [31] Joharapurkar AA, Dhanesha NA, Jain MR. Inhibition of the methionine aminopeptidase 2 enzyme for the treatment of obesity. *Diabetes Metab Syndr Obes.* **2014**;7:73.
- [32] Scroyen I, Christiaens V, Lijnen H. Effect of fumagillin on adipocyte differentiation and adipogenesis. *Biochim Biophys Acta.* **2010**;1800(4):425–429.
- [33] Lijnen HR, Frederix L, Van Hoef B. Fumagillin reduces adipose tissue formation in murine models of nutritionally induced obesity. *Obesity (Silver Spring).* **2010**;18(12):2241–2246.
- [34] White HM, Acton AJ, Considine RV. The angiogenic inhibitor TNP-470 decreases caloric intake and weight gain in high-fat fed mice. *Obesity (Silver Spring).* **2012**;20(10):2003–2009.
- [35] Tansey JT, Sztalryd C, Hlavin EM, et al. The central role of perilipin a in lipid metabolism and adipocyte lipolysis. *IUBMB Life.* **2004**;56(7):379–385.
- [36] Darlington GJ, Ross SE, MacDougald OA. The role of C/EBP genes in adipocyte differentiation. *J Biol Chem.* **1998**;273(46):30057–30060.
- [37] Rosen ED. The transcriptional basis of adipocyte development. *Prostaglandins, Leukotrienes Essent Fatty Acids.* **2005**;73(1):31–34.
- [38] Wu Z, Xie Y, Morrison RF, et al. PPARgamma induces the insulin-dependent glucose transporter GLUT4 in the absence of C/EBPalpha during the conversion of 3T3 fibroblasts into adipocytes. *J Clin Invest.* **1998**;101(1):22–32.
- [39] Wang H, Scott R. Inhibition of distinct steps in the adipocyte differentiation pathway in 3T3 T mesenchymal stem cells by dimethyl sulphoxide (DMSO). *Cell Prolif.* **1993**;26(1):55–66.
- [40] Vogel C, Marcotte EM. Insights into the regulation of protein abundance from proteomic and transcriptomic analyses. *Nat Rev Genet.* **2012**;13(4):227–232.
- [41] Burkey BF, Hoglen NC, Inskeep P, et al. Preclinical efficacy and safety of the novel antidiabetic, antiobesity MetAP2 inhibitor ZGN-1061. *J Pharmacol Exp Ther.* **2018**;365(2):301–313.